CLEO 2017

QELS-Fundamental Science, FTu3H.3: Active Plasmonics and Nanophotonics

14-19 May, 2017 – San Jose, California, USA

Laser Science to Photonic Applications

Modeling Nonlinear Resonators Comprising Graphene: A Coupled Mode Theory Approach

Thomas Christopoulos[1], Odysseas Tsilipakos[2], Nikolaos Grivas[1], Georgios Sinatkas[1], and Emmanouil E. Kriezis[1]

[1]*Dept. of Electrical and Computer Engineering, Aristotle University of Thessaloniki*

[2]*Inst. of Electronic Structure and Laser, Foundation for Research and Technology Hellas*

www.photonics.ee.auth.gr

Motivation and objectives

Motivation

- Exploit graphene's unique properties in practical nanophotonic resonators
  - Complex linear surface conductivity → strongly-confined modes
  - Highly dispersive
  - Highly nonlinear, Kerr-type response → low power nonlinear actions
- Expand perturbation theory and coupled mode theory framework to dispersive 2D sheet materials for efficient and accurate simulations

Objectives

- Physically model graphene as infinitesimally-thin (2D) material
- Obtain clear design rules for optical bistability in resonant structures
- Propose practical components in NIR and FIR (THz) regimes

Presentation outline

- **Mathematical Framework**
  - Perturbation Theory
  - Energy density in media with imaginary conductivity
  - Coupled Mode Theory
  - Application to optical bistability
- **Graphene Properties**
  - Far-Infrared regime (THz)
  - Near-Infrared regime
- **Resonant Structures**
  - 2D graphene-tube ring resonator (THz)
  - 3D graphene nanoribbon ring resonator (THz)
  - 3D silicon-slot ring resonator incorporating graphene (NIR)
- **Conclusion**

CLEO

Laser Science to Photonic Applications

Mathematical Framework

Perturbation Theory

Nonlinear frequency shift (perturbation theory)

Classic form: $$\frac{\Delta\omega}{\omega_0} = -\frac{1}{2}\frac{\iiint_V (\Delta\bar{\varepsilon}_r \mathbf{E_0}) \cdot \mathbf{E_0^*} \mathrm{d}V}{\iiint_V \bar{\varepsilon}_r \mathbf{E_0} \cdot \mathbf{E_0^*} \mathrm{d}V}$$ [*Bravo-Abad, JLT 25, 2539*]

Extended form: $$\frac{\Delta\omega}{\omega_0} = -\frac{\iiint_V \mathbf{P_{NL}} \cdot \mathbf{E_0^*} \mathrm{d}V - j\frac{1}{\omega_0}\iiint_V \mathbf{J_{NL}} \cdot \mathbf{E_0^*} \mathrm{d}V}{\iiint_V \varepsilon_0 \frac{\partial\{\omega\bar{\varepsilon}_r\}}{\partial\omega} \mathbf{E_0} \cdot \mathbf{E_0^*} \mathrm{d}V + \iiint_V \mu_0 \mathbf{H_0} \cdot \mathbf{H_0^*} \mathrm{d}V + \iiint_V \frac{\partial\bar{\sigma}_{\mathrm{Im}}^{(1)}}{\partial\omega} \mathbf{E_0} \cdot \mathbf{E_0^*} \mathrm{d}V}$$

[*Christopoulos, PRE 94, 062219*]

- Polarization nonlinearities
- Current density nonlinearities → Allows for modeling graphene
- Dispersive electric energy
- Extra energy term in media with dispersive complex conductivity
- Magnetic energy in the denominator ($W_e \neq W_m$; next slide)

Energy density in media with complex conductivity

Poynting theorem in the time domain

$$\langle \mathcal{J}(t)\cdot\mathcal{E}(t)\rangle = \underbrace{\frac{1}{2}\bar{\sigma}_{\mathrm{Re}}^{(1)}\mathbf{E_0}(\omega)\cdot\mathbf{E_0^*}(\omega)}_{\text{Power loss density}} + \frac{\partial}{\partial t}\underbrace{\left\{\frac{1}{4}\frac{\partial\bar{\sigma}_{\mathrm{Im}}^{(1)}}{\partial\omega}\mathbf{E_0}(\omega)\cdot\mathbf{E_0^*}(\omega)\right\}}_{\text{Stored energy density}}$$

Zero when dispersion is neglected

Energy density in media with complex conductivity

Poynting theorem in the time domain

$$\langle \mathcal{J}(t)\cdot\mathcal{E}(t)\rangle = \underbrace{\frac{1}{2}\bar{\sigma}_{\mathrm{Re}}^{(1)}\mathbf{E_0}(\omega)\cdot\mathbf{E_0^*}(\omega)}_{\text{Power loss density}} + \underbrace{\frac{\partial}{\partial t}\left\{\frac{1}{4}\frac{\partial\bar{\sigma}_{\mathrm{Im}}^{(1)}}{\partial\omega}\mathbf{E_0}(\omega)\cdot\mathbf{E_0^*}(\omega)\right\}}_{\text{Stored energy density}}$$

Zero when dispersion is neglected

Poynting theorem in the frequency domain

$$-\iiint_V \nabla\cdot\mathbf{S}\mathrm{d}V = \frac{1}{2}\iiint_V \bar{\sigma}_{\mathrm{Re}}^{(1)}\mathbf{E_0}\cdot\mathbf{E_0^*}\mathrm{d}V -$$

$$-j\frac{1}{2}\omega_0\iiint_V \varepsilon_0\bar{\varepsilon}_r\mathbf{E_0}\cdot\mathbf{E_0^*}\mathrm{d}V + j\frac{1}{2}\omega_0\iiint_V \mu_0\mathbf{H_0}\cdot\mathbf{H_0^*}\mathrm{d}V + j\frac{1}{2}\iiint_V \bar{\sigma}_{\mathrm{Im}}^{(1)}\mathbf{E_0}\cdot\mathbf{E_0^*}\mathrm{d}V$$

$$= P_{\mathrm{loss}} + j\left(-Q_E + Q_H + Q_J\right)$$

- Reactive power ≠ Dispersive energy ($Q \neq 2\omega_0 W$)
- On resonance:
  - $Q_E = Q_H + Q_J$
  - $W_e \neq W_m$ (equality typically taken for granted)

Coupled Mode Theory (CMT)

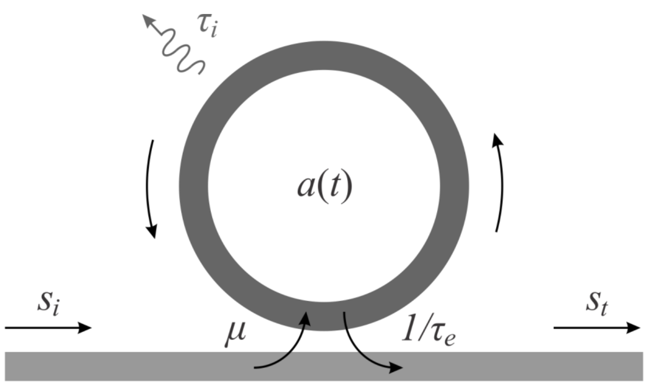

$$\frac{\mathrm{d}a}{\mathrm{d}t} = j(\omega_0 + \Delta\omega)a - \left(\frac{1}{\tau_i} + \frac{1}{\tau_e}\right)a + \mu s_i$$

$$s_t = s_i + \mu a$$

$\alpha(t)$	cavity amplitude, $\lvert a\rvert^2 \equiv W_e + W_m + W_j$
ω_0	unperturbed resonance frequency
$\Delta\omega$	nonlinear frequency shift
τ	photon lifetime, $\tau = 2Q/\omega_0$
μ	coupling coefficient, $\mu = j\sqrt{2/\tau_e}$
$s(t)$	w/g mode amplitude, $\lvert s\rvert^2 \equiv P$

[*Tsilipakos, JOSA B 31, 2014*]
[*Soljacic, PRE 5, 2002*]

Steady-state response

$$\frac{p_{\text{out}}}{p_{\text{in}}} = \frac{(\delta + p_{\text{in}} - p_{\text{out}})^2 + \left(1 - r_Q\right)^2}{(\delta + p_{\text{in}} - p_{\text{out}})^2 + \left(1 + r_Q\right)^2}$$

$\delta = \tau_i(\omega - \omega_0)$	normalized detuning
$\delta_{\text{th}} = -\left(1 + r_Q\right)\sqrt{3}$	detuning threshold for BI
$r_Q = Q_i/Q_e$	quality factor ratio
$p = P/P_0$	normalized power
P_0	characteristic power

- Closed-form polynomial equation
- Admits three real positive solutions (optical bistability)
  - $\delta < \delta_{\text{th}}$ or $\delta > -\delta_{\text{th}}$
  - $P_{\text{in}} > 5P_0$
- Minimize $P_0 \propto 1/(Q^2\kappa)$
- Critical coupling condition, $r_Q = 1$

CLEO

Photonics Group | Dept. of ECE | AUTH
www.photonics.ee.auth.gr

Application to optical bistability

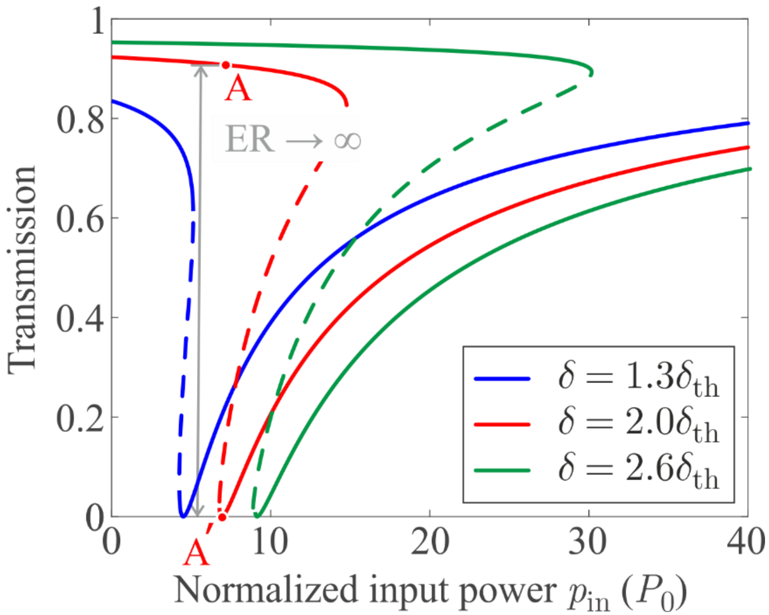

Increase in |δ|

- ✗ Higher input power required
- ✓ Loop span increases
- ✓ Maximum transmission increases

Application to optical bistability

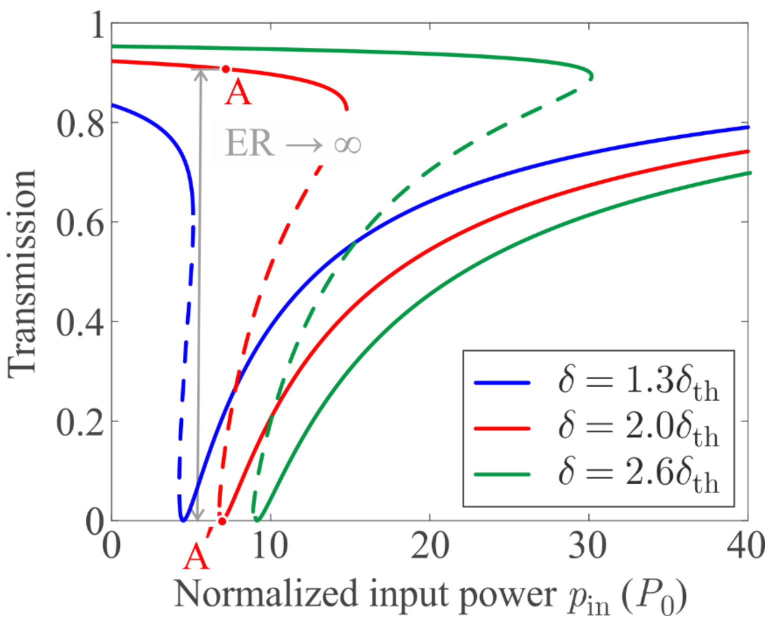

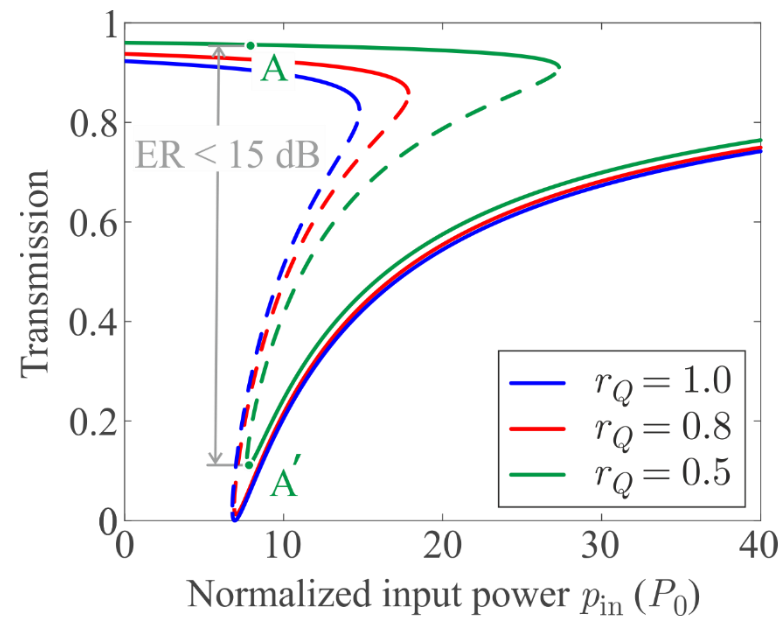

Increase in $|\delta|$

- ✗ Higher input power required
- ✓ Loop span increases
- ✓ Maximum transmission increases

Decreasing r_Q below 1

- ✗ Higher input power required
- ✗ T_{min} increases (loop elevation)
- ✓ Loop span increases (δ_{th} decreases)

CLEO

Photonics Group | Dept. of ECE | AUTH
www.photonics.ee.auth.gr

Application to optical bistability

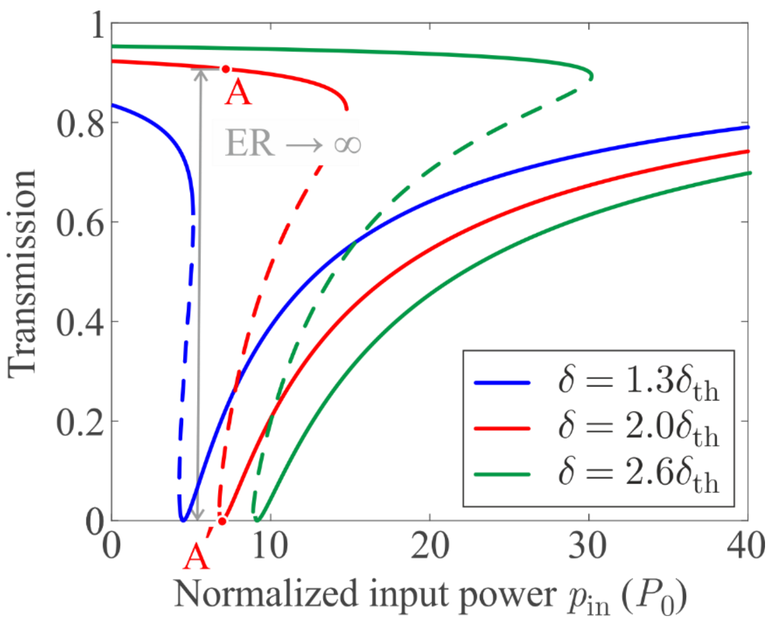

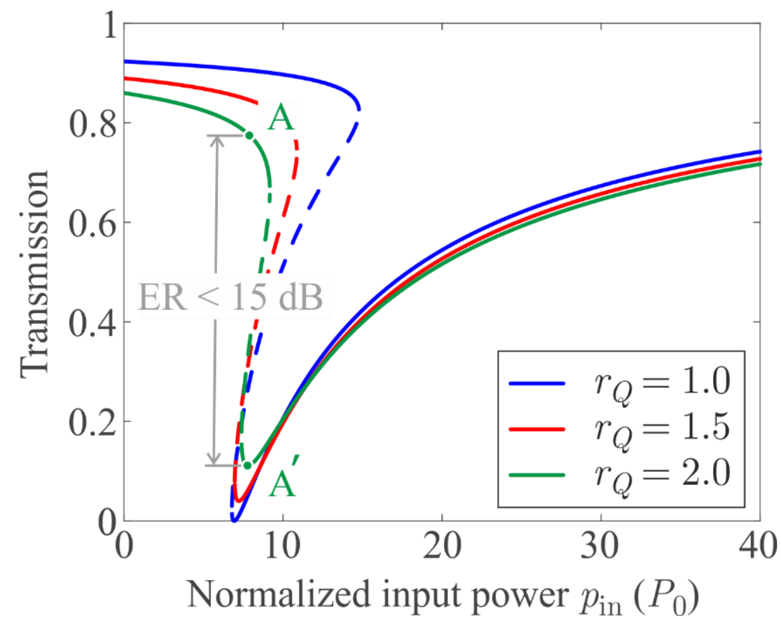

Increase in $|\delta|$

- × Higher input power required
- ✓ Loop span increases
- ✓ Maximum transmission increases

Decreasing r_Q below 1

- × Higher input power required
- × T_{min} increases (loop elevation)
- ✓ Loop span increases (δ_{th} decreases)

Increasing r_Q above 1

- × Higher input power required
- × T_{min} increases (loop elevation)
- × Loop span decreases (δ_{th} increases)

CLEO

Laser Science to Photonic Applications

Graphene Properties

Far-Infrared regime (THz)

Linear Properties

$$\mathbf{J}_{s,\mathrm{lin}} = \sigma_{\mathrm{intra}}(\omega)\mathbf{E}_{0,\parallel}$$

- Only intraband transitions allowed (Drude-like response)
- Complex electrical conductivity $\sigma_1 = \sigma_{\mathrm{intra}}$
  - Small $\mathrm{Re}\{\sigma_1\}$ (low losses)
  - Highly negative $\mathrm{Im}\{\sigma_1\}$ (plasmonic behavior)
- Strong dispersion

[*Falkovsky, Phys. Usp. 178, 887*]

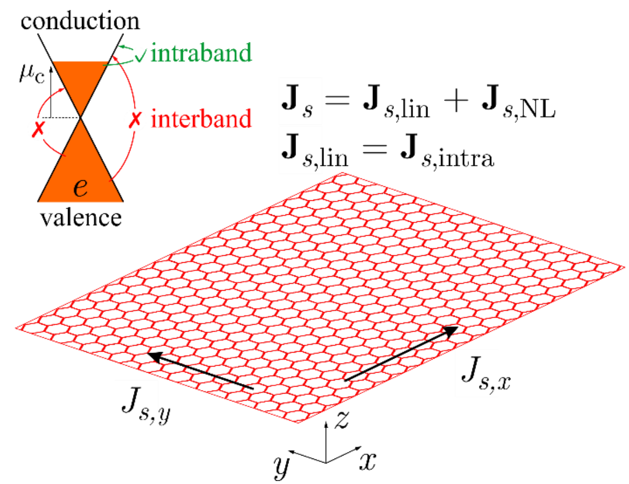

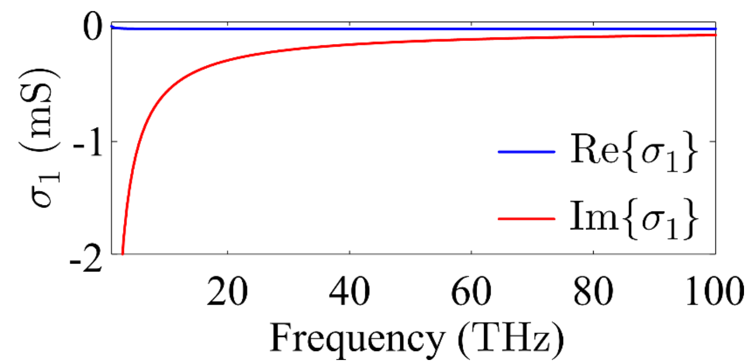

Nonlinear Properties

$$\mathbf{J}_{s,\mathrm{NL}} = \frac{\sigma_3(\omega)}{4}\left[2\left(\mathbf{E}_{0,\parallel}\cdot\mathbf{E}_{0,\parallel}^*\right)\mathbf{E}_{0,\parallel} + \left(\mathbf{E}_{0,\parallel}\cdot\mathbf{E}_{0,\parallel}\right)\mathbf{E}_{0,\parallel}^*\right]$$

- Kerr-type nonlinearity (purely imaginary σ_3)
- $\sigma_3 = j4.7\times10^{-19}\ \mathrm{S(m/V)^2}$ @ $10\ \mathrm{THz}$
- $n_2^{\mathrm{eq}} = 2.4\times10^{-13}\ \mathrm{m^2/W}$ (self-focusing material)

[*Mikhailov, J. Phys.: Condenc. Matter 20, 384204*]

Near-Infrared regime (NIR)

Linear Properties

$$\mathbf{J}_{s,\text{lin}} = \big(\sigma_{\text{intra}}(\omega) + \sigma_{\text{inter}}(\omega)\big)\mathbf{E}_{0,\parallel}$$

- Intraband transitions always allowed
- Interband transitions allowed for $hf < 2\mu_c$
- Low loss regime $\mu_c \approx 0.4$ eV @ $\lambda = 1.55$ μm (0.8 eV)
- Mild dispersion

[*Hanson, IEEE Trans. Ant. Propag. 56, 064302*]

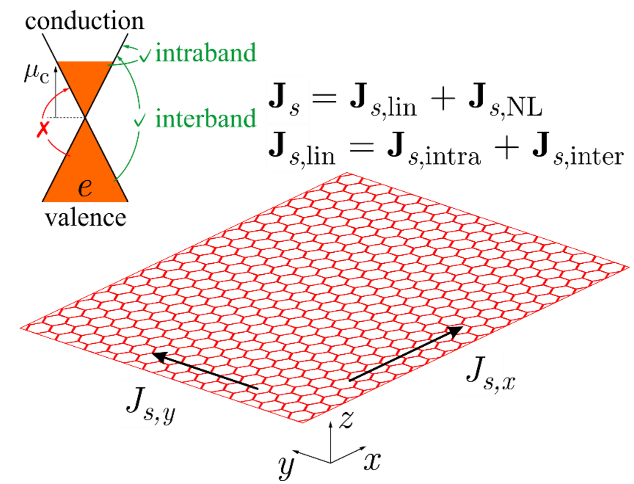

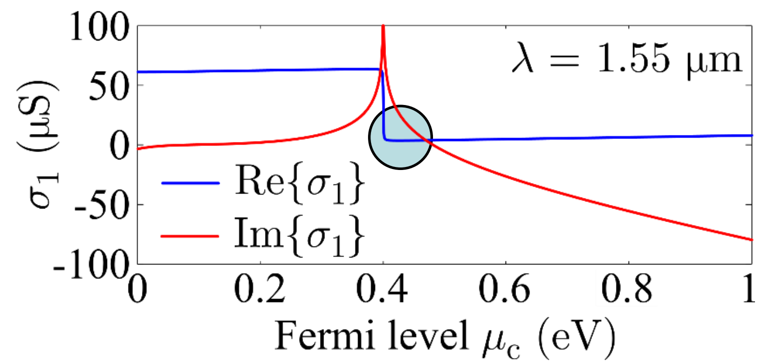

Nonlinear Properties

$$\mathbf{J}_{s,\text{NL}} = \frac{\sigma_3(\omega)}{4}\left[2\big(\mathbf{E}_{0,\parallel}\cdot\mathbf{E}^*_{0,\parallel}\big)\mathbf{E}_{0,\parallel} + \big(\mathbf{E}_{0,\parallel}\cdot\mathbf{E}_{0,\parallel}\big)\mathbf{E}^*_{0,\parallel}\right]$$

- Kerr-type nonlinearity (purely imaginary σ_3)
- $n_2^{\text{eq}} = -1\times10^{-13}$ m^2/W (defocusing material)
- $\sigma_3 = -j5.5\times10^{-21}$ S(m/V)^2 @ 1.55 μm

[*Dremetsika, Opt. Lett. 41, 3281*]
[*Vermeulen, PRA 6, 044006*]

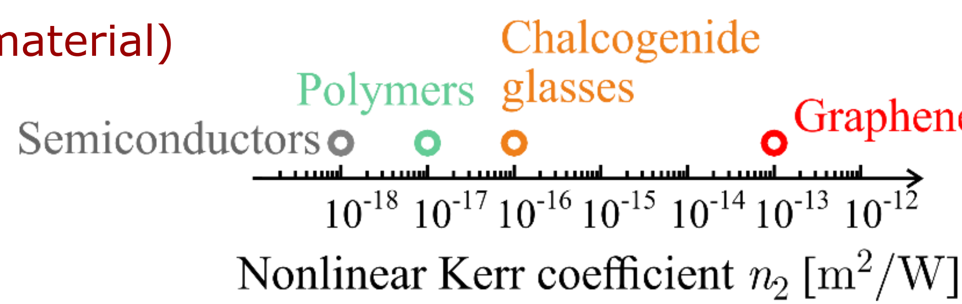

CLEO

Laser Science to Photonic Applications

Resonant Structures

2D graphene-tube ring resonator (1)

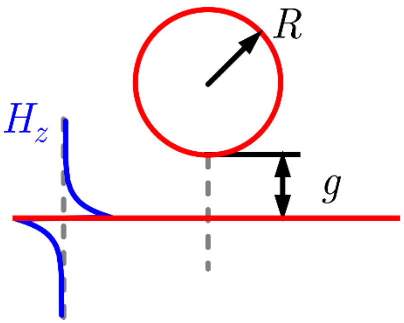

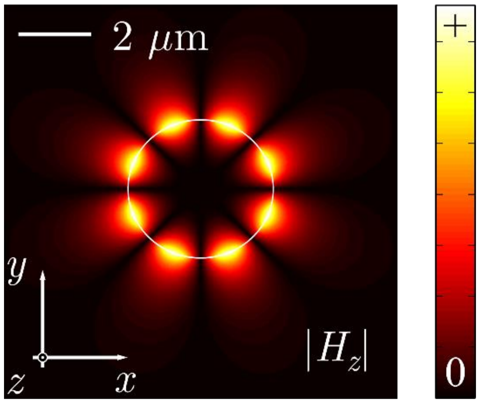

- ○ Resonator: Infinite graphene tube
- ○ Bus waveguide: Infinite graphene sheet
- ✓ Surface Plasmon Polaritons supported at THz
  - Sub-wavelength confinement
  - Low radiation losses
  - Low-power, Kerr-induced bistability

Nonlinear frequency shift

$$\Delta\omega = \left(\frac{\omega_0}{c_0}\right)^3 \kappa_s \frac{\sigma_{3,\mathrm{Im}}^{\max}}{\varepsilon_0^2}\left(W_e + W_m + W_j\right)$$

Characteristic Power

$$\boxed{P_0 = \frac{\varepsilon_0^2 c_0^3}{2\omega_0 \sigma_{3,\mathrm{Im}}^{\max} \kappa_s Q_i^2} \propto \frac{1}{\kappa_s Q_i^2}}$$

P_0 must be minimized for optimum performance

[*Christopoulos, PRE 94, 062219*]
[*Tsilipakos, JLT 34, 1333*]

Nonlinear feedback parameter

$$\boxed{\kappa_s = \left(\frac{c_0}{\omega_0}\right)^3 \frac{\int_l \sigma_{3,\mathrm{Im}}\left(2\left|\mathbf{E}_{0,\parallel}\right|^4 + \left|\mathbf{E}_{0,\parallel}\cdot\mathbf{E}_{0,\parallel}\right|^2\right)\mathrm{d}l}{\left[\iint_S \varepsilon_r |\mathbf{E}_0|^2 \mathrm{d}S + \iint_S \eta_0^2 |\mathbf{H}_0|^2 \mathrm{d}S + \frac{1}{\varepsilon_0}\int_l \frac{\partial \sigma_{1,\mathrm{Im}}}{\partial\omega}\left|\mathbf{E}_{0,\parallel}\right|^2 \mathrm{d}l\right]^2 \sigma_{3,\mathrm{Im}}^{\max}}}$$

CLEO

2D graphene-tube ring resonator (2)

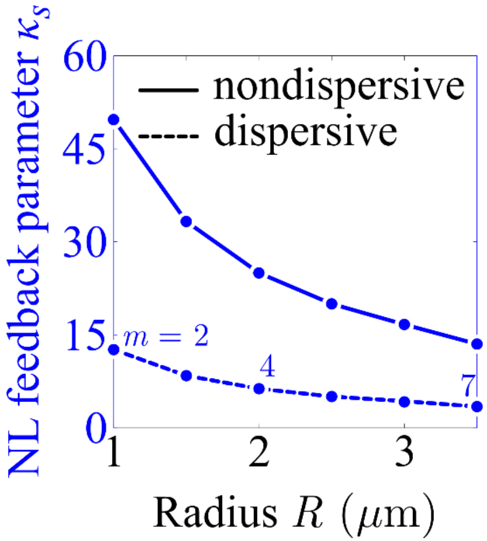

- $\kappa_s \propto 1/R$
- $\kappa_s^{\mathrm{non}} \approx 4\kappa_s^{\mathrm{disp}}$

CLEO

Photonics Group | Dept. of ECE | AUTH
www.photonics.ee.auth.gr

2D graphene-tube ring resonator (2)

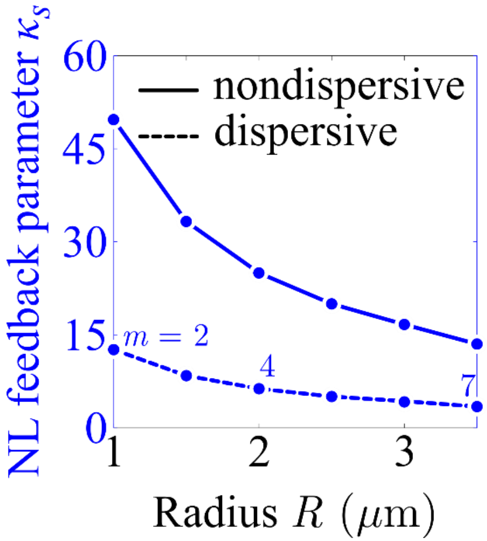

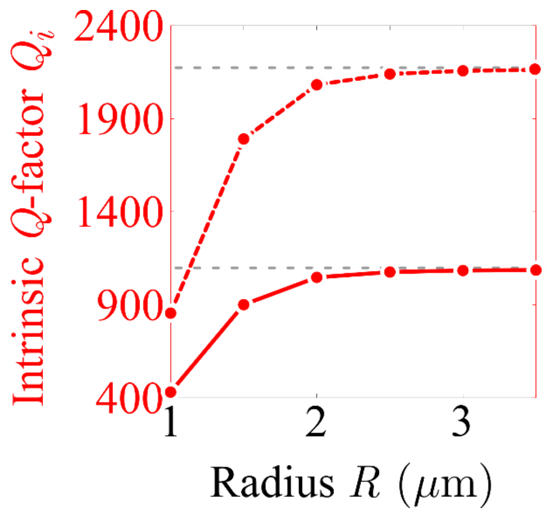

- $\kappa_s \propto 1/R$
- $\kappa_s^{\text{non}} \approx 4\kappa_s^{\text{disp}}$

- $Q_i \propto R$
- $Q_i^{\text{disp}} \approx 2Q_i^{\text{non}}$

2D graphene-tube ring resonator (2)

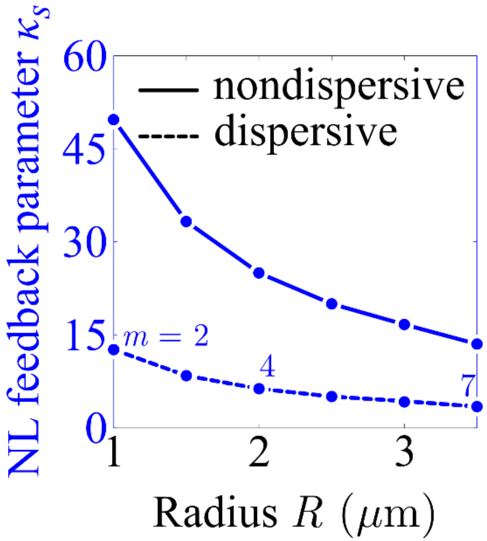

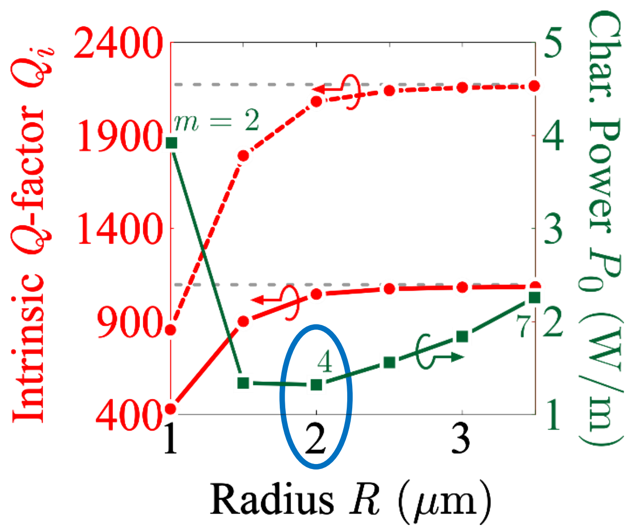

- $\kappa_s \propto 1/R$
- $\kappa_s^{\mathrm{non}} \approx 4\kappa_s^{\mathrm{disp}}$

- $Q_i \propto R$
- $Q_i^{\mathrm{disp}} \approx 2Q_i^{\mathrm{non}}$

- $R = 2\ \mu\mathrm{m}$
- $g = 1.74\ \mu\mathrm{m}$
- $P_0 = 1.32\ \mathrm{W/m}$
- $P_{0,\mathrm{eq}}^{3\mathrm{D}} \approx 20\ \mu\mathrm{W}$
- $f_0 = 10.021\ \mathrm{THz}$

- P_0 is the same since $\kappa_s^{\mathrm{non}}(Q_i^{\mathrm{non}})^2 = \kappa_s^{\mathrm{disp}}\left(Q_i^{\mathrm{disp}}\right)^2$
- Total minimum of P_0 for low-power bistability
- Critical coupling $[r_Q = 1]$

CLEO

2D graphene-tube ring resonator (3)

CW case

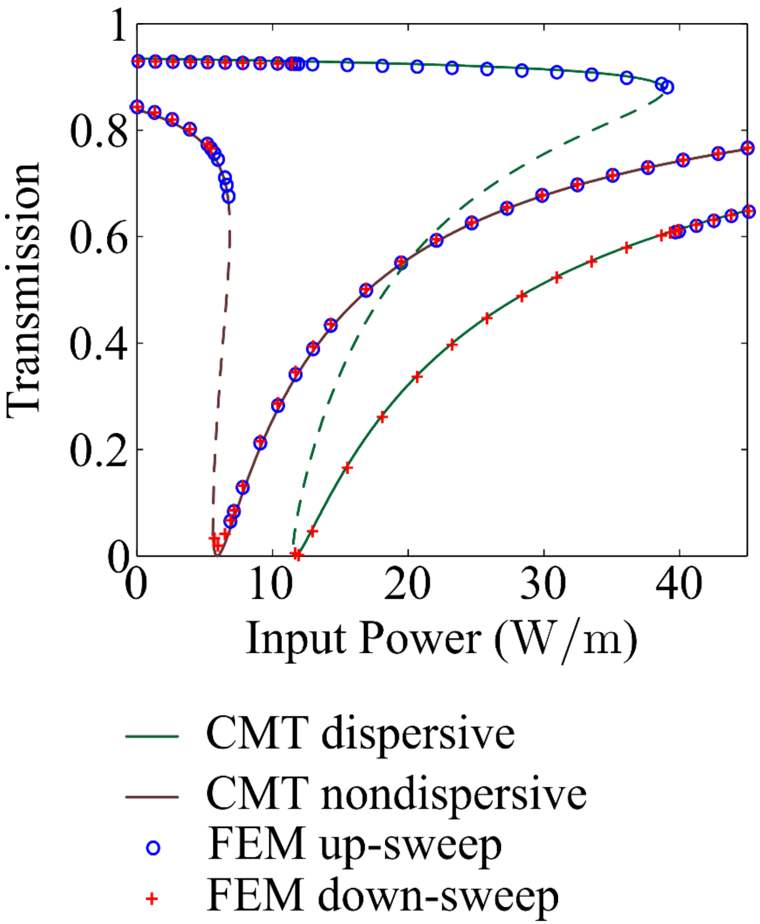

- CMT
  - $Q_i^{\text{disp}} \approx 2Q_i^{\text{non}} \Longrightarrow \delta^{\text{disp}} = 2\delta^{\text{non}}$
  - ✓ Always include dispersion
- NL-VFEM
  - Two power sweeps (ascending and descending)
  - Initial condition of each step: previous solution
  - ✓ Excellent agreement between FEM and CMT

CLEO

2D graphene-tube ring resonator (3)

CW case

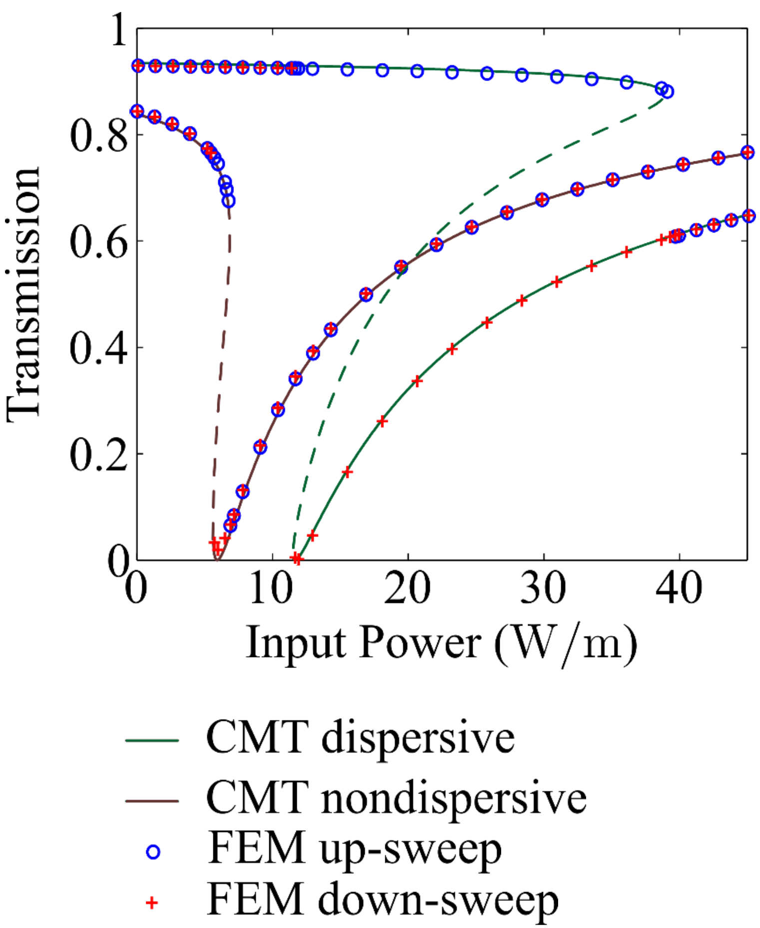

- CMT
  - $Q_i^{\mathrm{disp}} \approx 2Q_i^{\mathrm{non}} \Longrightarrow \delta^{\mathrm{disp}} = 2\delta^{\mathrm{non}}$
  - ✓ Always include dispersion
- NL-VFEM
  - Two power sweeps (ascending and descending)
  - Initial condition of each step: previous solution
  - ✓ Excellent agreement between FEM and CMT

Dynamic memory implementation

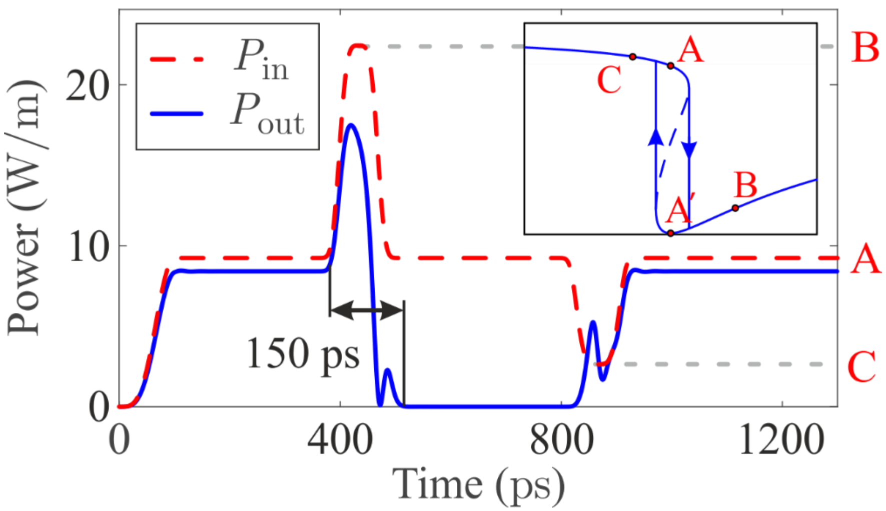

3D graphene nanoribbon ring resonator

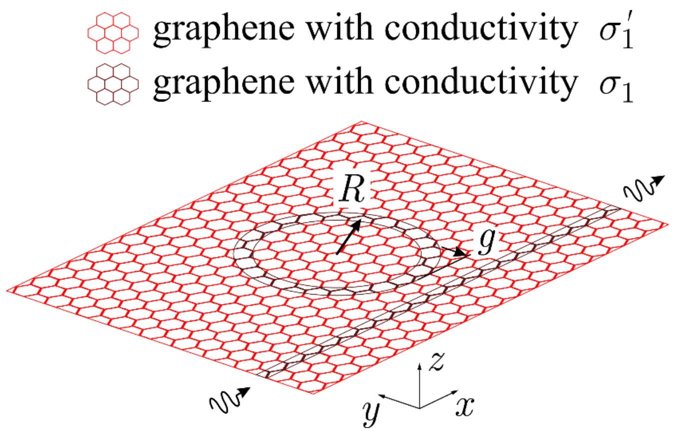

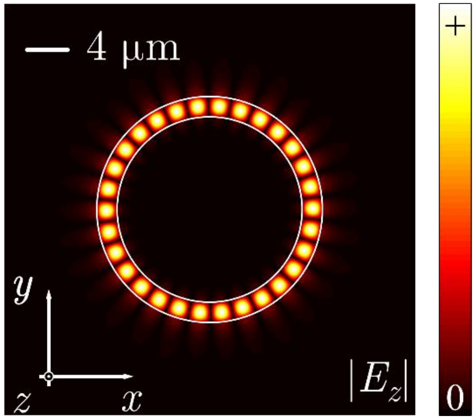

- Infinite graphene sheet
- Resonator/waveguide:
  - "Written" with $|\sigma_{1,\mathrm{Im}}| < |\sigma'_{1,\mathrm{Im}}|$
  - Uneven ground and/or voltage
- ✓ Surface Plasmon Polariton supported at THz

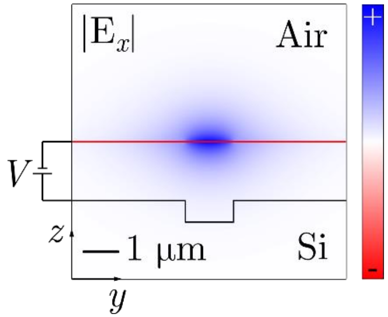

- $R = 10.1$ µm
- $g = 2.20$ µm
- $P_0 = 24$ µW
- $f_0 = 10$ THz

- $Q_i^{\mathrm{non}} = 1048$
- $Q_i^{\mathrm{disp}} = 2080$
- $\kappa_s^{\mathrm{non}} = 6.52$
- $\kappa_s^{\mathrm{disp}} = 1.65$

[*Vakil and Engheta, Science 332, 1291*]

3D silicon-slot ring resonator incorporating graphene

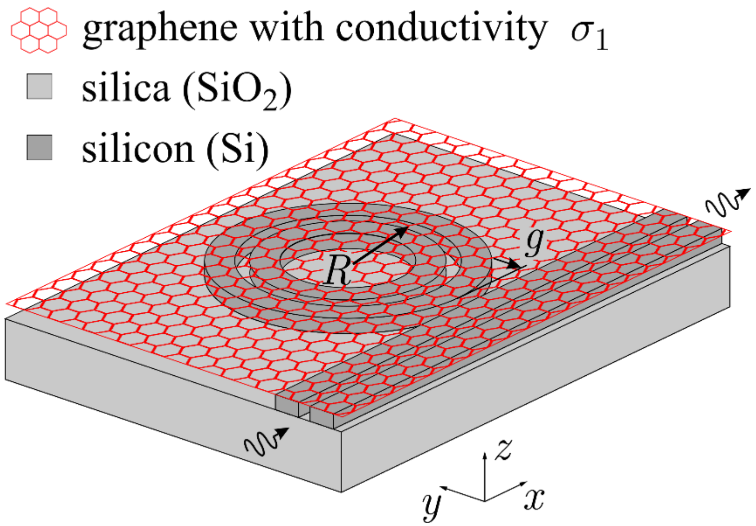

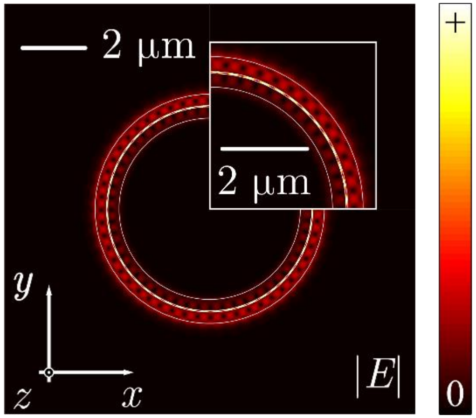

- Si-slot platform
  - High confinement
  - Major E-field component ∥ to graphene
- Infinite graphene sheet on top

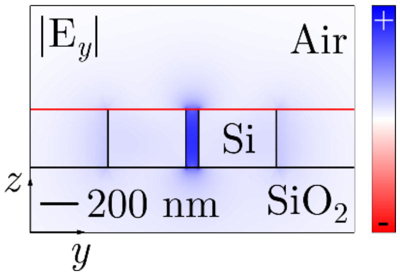

- $R = 3.25$ µm
- $g = 150$ nm
- $P_0^{\mathrm{Kerr}} = 6.2$ mW
- $\lambda_0 = 1.553$ µm

- $P_{0,s}^{\mathrm{Kerr}} = 6.1$ mW
- $P_{0,b}^{\mathrm{Kerr}} = 1.6$ W

Conclusion

Summary

- Strict framework for nonlinear resonators comprising bulk (3D) and/or sheet (2D) dispersive material
- Rigorous design rules for low-power bistability
- Excellent agreement with full-wave simulations
- Practical 3D nanophotonic components in both NIR and FIR (THz) regimes
- Opens the way for switching, memory, and logic applications

To probe further …

- Incorporate Two Photon Absorption in graphene
- Exploit the framework for multi-channel non-linear actions
  - Two-channel $\chi^{(3)}$ effects: Cross-Phase Modulation, Third Harmonic Generation
  - Three-channel $\chi^{(3)}$ effects: Degenerated Four-Wave Mixing
- Dynamic control via graphene's free carriers (μ_c tuning)

Thank you!

web: www.photonics.ee.auth.gr
e-mail: cthomasa@ece.auth.gr

*This work was supported by the "**Research Projects for Excellence, IKY/SIEMENS**".*

And… there is more

Back up material !

Energy density in media with complex conductivity (full proof)

- Poynting vector in time domain: $-\nabla\cdot\boldsymbol{\mathcal{S}} = -\nabla\cdot(\boldsymbol{\mathcal{E}}\times\boldsymbol{\mathcal{H}}) = \boldsymbol{\mathcal{J}}\cdot\boldsymbol{\mathcal{E}} + \frac{\partial\boldsymbol{\mathcal{D}}}{\partial t}\cdot\boldsymbol{\mathcal{E}} + \frac{\partial\boldsymbol{\mathcal{B}}}{\partial t}\cdot\boldsymbol{\mathcal{H}}$
- Second and third terms correspond to stored energy. What about the first term?

- Slow varying envelope: $\boldsymbol{\mathcal{F}} = \mathrm{Re}\{\mathbf{F}_0\exp(+j\omega_0 t)\} = (\mathbf{F}_0+\mathbf{F}_0^*)/2\,,\qquad \boldsymbol{\mathcal{F}} = \{\boldsymbol{\mathcal{E}},\boldsymbol{\mathcal{J}}\}$
- Time averaging w.r.t. $T_0 = 2\pi/\omega_0$: $\langle\boldsymbol{\mathcal{J}}\cdot\boldsymbol{\mathcal{E}}\rangle = (\mathbf{E}_0^*\cdot\mathbf{J}_0 + \mathbf{E}_0\cdot\mathbf{J}_0^*)/4$
- Fourier transform on the envelope: $\mathbf{J}_0(t) = \frac{1}{2\pi}\int\tilde{\mathbf{J}}_0(\omega)e^{j\omega t}\,\mathrm{d}\omega$
- Apply Ohm's law to the "high" frequency: $\tilde{\mathbf{J}}_0(\omega) = \bar{\sigma}^{(1)}(\omega+\omega_0)\tilde{\mathbf{E}}_0(\omega)$
- Expand $\bar{\sigma}^{(1)}$ in Taylor series: $\begin{cases}\bar{\sigma}_{\mathrm{Re}}^{(1)}(\omega+\omega_0)\approx\bar{\sigma}_{\mathrm{Re}}^{(1)}(\omega_0)\\ \bar{\sigma}_{\mathrm{Im}}^{(1)}(\omega+\omega_0)\approx\bar{\sigma}_{\mathrm{Im}}^{(1)}(\omega_0)+\omega\left.\frac{\partial\bar{\sigma}_{\mathrm{Im}}^{(1)}}{\partial\omega}\right|_{\omega=\omega_0}\end{cases}$
- Inverse Fourier transform on the result
- Finally:

$$\langle\boldsymbol{\mathcal{J}}\cdot\boldsymbol{\mathcal{E}}\rangle = \underbrace{\frac{1}{2}\bar{\sigma}_{\mathrm{Re}}^{(1)}\mathbf{E_0}\cdot\mathbf{E_0^*}}_{\text{Power loss density}} + \frac{\partial}{\partial t}\underbrace{\left\{\frac{1}{4}\frac{\partial\bar{\sigma}_{\mathrm{Im}}^{(1)}}{\partial\omega}\mathbf{E_0}\cdot\mathbf{E_0^*}\right\}}_{\text{Stored energy density}}$$

[*Landau and Lifshitz, Electrodynamics of continuous media, Elsevier, 1984*]

[*Christopoulos, PRE 94, 062219*]

Correct calculation of κ

FEM eigenvalue solution

- Two degenerated counter-propagating modes
- Standing-wave pattern
- $\mathbf{E}(\rho,\varphi) = \mathbf{e}^{+}(\rho,\varphi) + \mathbf{e}^{-}(\rho,\varphi)$
- $\mathbf{H}(\rho,\varphi) = \mathbf{h}^{+}(\rho,\varphi) + \mathbf{h}^{-}(\rho,\varphi)$

FEM propagation solution

- One single mode propagating (counter)clockwise
- Traveling-wave pattern
- $\mathbf{E}(\rho,\varphi) = \mathbf{e}^{+}(\rho,\varphi)$
- $\mathbf{H}(\rho,\varphi) = \mathbf{h}^{+}(\rho,\varphi)$

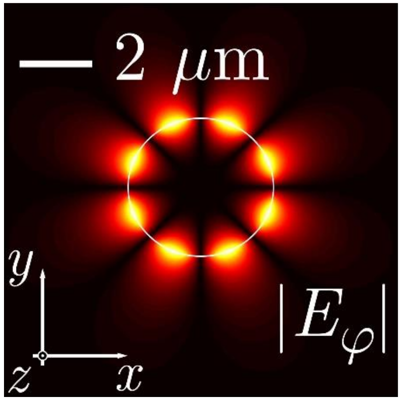

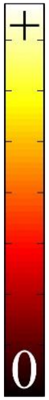

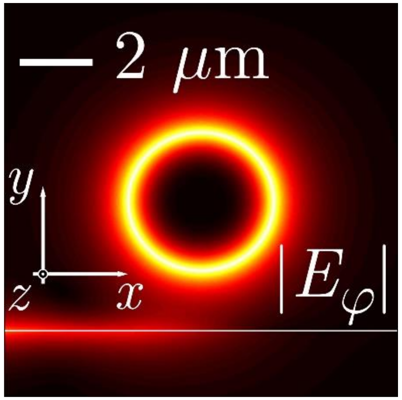

$$\mathbf{e}^{\pm}(\rho,\varphi) = \left[e_{\rho}(\rho)\hat{\boldsymbol{\rho}} \pm j e_{\rho}(\rho)\hat{\boldsymbol{\varphi}}\right]\exp\{\mp jm\varphi\}$$

$$\mathbf{h}^{\pm}(\rho,\varphi) = \mp h_z(\rho)\hat{\mathbf{z}}\exp\{\mp jm\varphi\}$$

$$\boxed{\frac{\kappa_s^{\mathrm{prop}}}{\kappa_s^{\mathrm{eig}}} = \frac{2}{3}}$$

3D graphene nanoribbon ring resonator

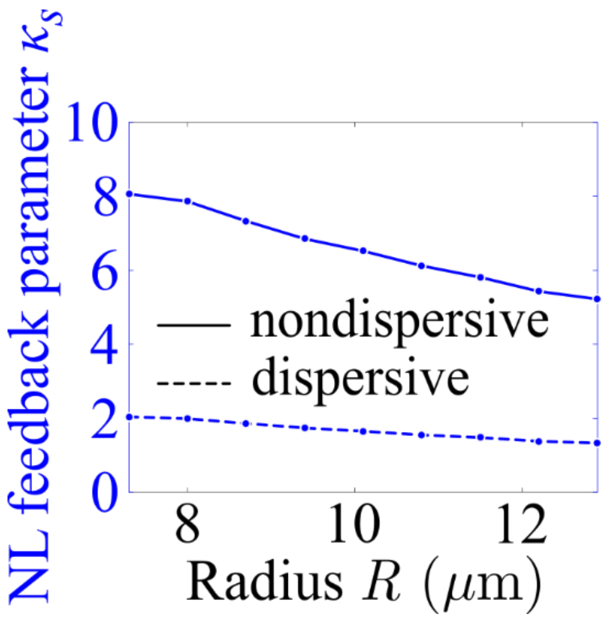

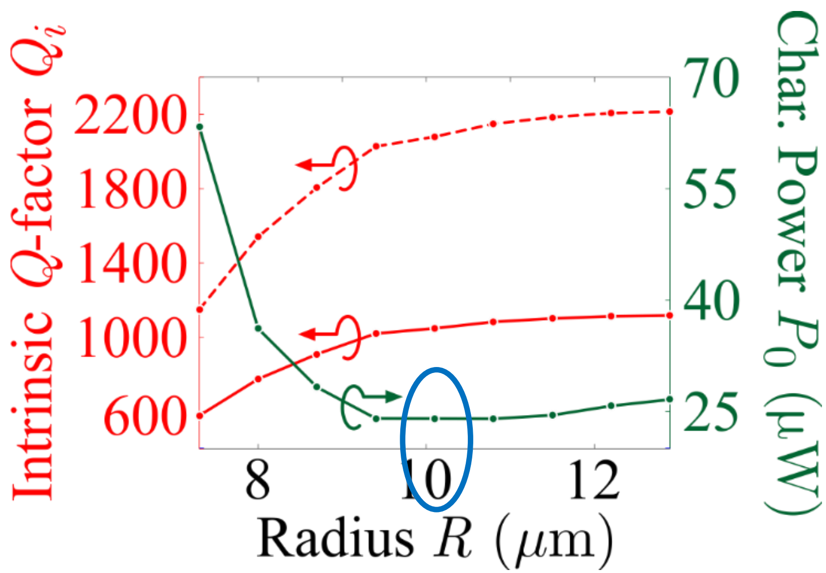

- $R = 10.1\ \mu\text{m}$
- $g = 2.20\ \mu\text{m}$
- $P_0 = 24\ \mu\text{W}$
- $f_0 = 10\ \text{THz}$

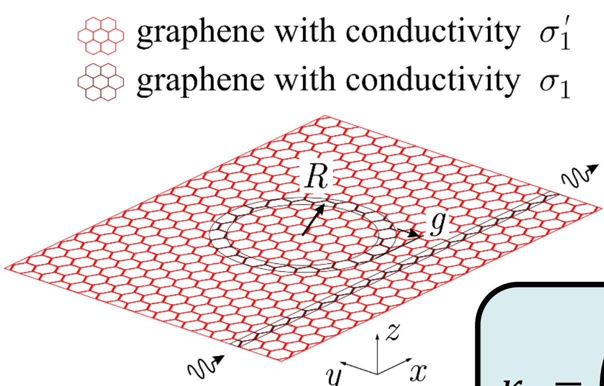

Nonlinear feedback parameter

$$\kappa_s = \left(\frac{c_0}{\omega_0}\right)^4 \frac{\iint_S \sigma_3 \left(2\left|\mathbf{E}_{0,\parallel}\right|^4 + \left|\mathbf{E}_{0,\parallel}\cdot\mathbf{E}_{0,\parallel}\right|^2\right) \mathrm{d}S}{\left[\iiint_V \varepsilon_r |\mathbf{E}_0|^2 \mathrm{d}V + \iiint_V \eta_0^2 |\mathbf{H}_0|^2 \mathrm{d}V + \frac{1}{\varepsilon_0}\iint_S \frac{\partial\sigma_{1,\mathrm{Im}}}{\partial\omega}\left|\mathbf{E}_{0,\parallel}\right|^2 \mathrm{d}S\right]^2 \sigma_3^{\max}}$$

Photonics Group | Dept. of ECE | AUTH
www.photonics.ee.auth.gr

3D silicon-slot ring resonator incorporating graphene

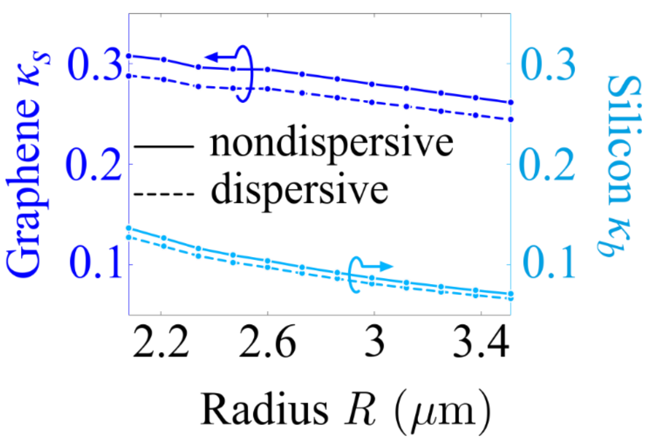

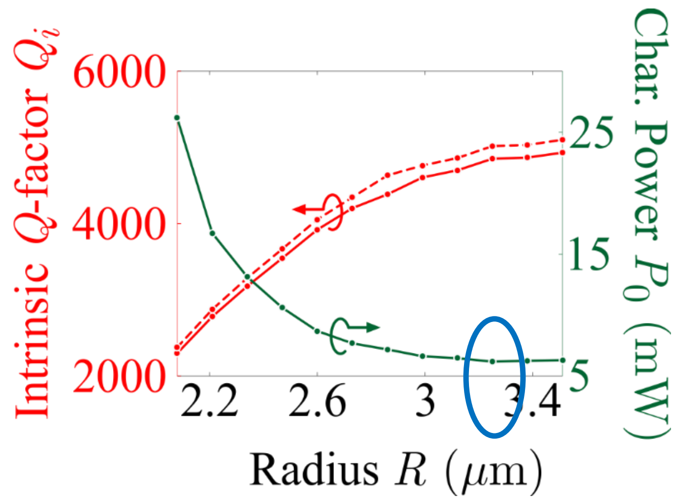

- $R = 3.25$ μm
- $g = 150$ nm
- $P_0 = 6.2$ mW
- $\lambda_0 = 1.553$ nm

Nonlinear feedback parameters

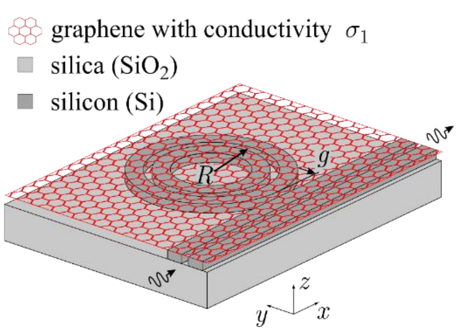

$$\kappa_s = \left(\frac{c_0}{\omega_0}\right)^4 \frac{\iint_S \sigma_3 \left(2\left|\mathbf{E}_{0,\parallel}\right|^4 + \left|\mathbf{E}_{0,\parallel}\cdot\mathbf{E}_{0,\parallel}\right|^2\right)\mathrm{d}S}{\left[\iiint_V \varepsilon_r|\mathbf{E}_0|^2\mathrm{d}V + \iiint_V \eta_0^2|\mathbf{H}_0|^2\mathrm{d}V + \frac{1}{\varepsilon_0}\iint_S \frac{\partial\sigma_{1,\mathrm{Im}}}{\partial\omega}\left|\mathbf{E}_{0,\parallel}\right|^2\mathrm{d}S\right]^2 \sigma_3^{\max}}$$

$$\kappa_b = \left(\frac{c_0}{\omega_0}\right)^3 \frac{\frac{1}{3}\iiint_V n^2 n_2 \left(2|\mathbf{E}_0|^4 + |\mathbf{E}_0\cdot\mathbf{E}_0|^2\right)\mathrm{d}V}{\left[\iiint_V \varepsilon_r|\mathbf{E}_0|^2\mathrm{d}V + \iiint_V \eta_0^2|\mathbf{H}_0|^2\mathrm{d}V + \frac{1}{\varepsilon_0}\iint_S \frac{\partial\sigma_{1,\mathrm{Im}}}{\partial\omega}\left|\mathbf{E}_{0,\parallel}\right|^2\mathrm{d}S\right]^2 n_2^{\max}}$$